

Marek Konieczny

Politechnika Świętokrzyska, Katedra Metaloznawstwa i Technologii Materiałowych, al. 1000-lecia P.P. 7, 25-314 Kielce, Poland
* Corresponding author. E-mail: mkon@interia.pl

Otrzymano (Received) 15.11.2010

COMPOSITE γ -Ni+ γ' /Ni COATINGS ON IRON TRANSFORMED FROM ELECTRODEPOSITED Ni AND SEDIMENT CO-DEPOSITED Ni+Al FILMS

Ni+Al/Ni composite coatings on an iron substrate were successfully developed via two-step technology: conventional electrodeposition (CED) and sediment co-deposition (SCD). The Al content produced in the composite coatings was about 25 vol. %. The coating morphology and composition were characterised using light optical microscopy, scanning electron microscopy (SEM - JEOL JMS 5400) and electron probe microanalysis (EDS - ISIS 300 Oxford Instruments). No cracking, porosity or other defects were observed in the Ni+Al/Ni coating microstructure. The hardness of the Ni+Al coating was about 240 HV, whereas the hardness of the pure Ni interlayer coating was only 220 HV. The effect of heat treatment under pressure on coating phase formation was studied. The Ni+Al/Ni coatings were converted into γ -Ni+ γ' /Ni coatings by vacuum annealing at 600°C for 2 h and subsequently at 900°C for 3 h under uniaxial pressure of 1 MPa. Full-density composite coatings were obtained. The nickel interlayer was successfully employed to block the mutual diffusion between the iron substrate and aluminium and therefore hard and brittle Fe-Al intermetallics were not formed. The hardness of the reaction-formed γ -Ni+ γ' layer was about 280 HV. The hardness near the surface after oxidation tests decreased to about 250 HV, which was attributed to the depletion of the γ' phase. A hardness peak of about 320 HV appeared about 15 μ m within the outer layer, where the alumina continuous layer was revealed. The results of the microindentation hardness measurements were in accordance with the results of the SEM and EDS analysis.

Keywords: γ -Ni/ γ' composite coating, sediment co-deposition, annealing, oxidation

WARSTWY KOMPOZYTOWE γ -Ni+ γ' /Ni NA PODŁOŻU ŻELAZA ARMCO WYTWARZANE NA DRODZE TRANSFORMACJI GALWANICZNYCH WARSTW Ni ORAZ Ni+Al

Warstwy kompozytowe Ni+Al/Ni na podłożu żelaza ARMCO zostały wytworzone metodą składającą się z dwóch etapów: konwencjonalnego osadzania galwanicznego warstw niklowych oraz współosadzania sedymentacyjnego warstw Ni+Al. Zawartość aluminium w osadzanych warstwach wynosiła około 25% objętości. Morfologia oraz skład uzyskanych warstw były badane przy użyciu mikroskopu optycznego NEOPHOT 2, mikroskopu skaningowego JEOL JMS 5400 oraz mikroanalityzatora rentgenowskiego ISIS 300 Oxford Instruments. Podczas obserwacji uzyskanych warstw Ni+Al/Ni nie stwierdzono występowania pęknięć, porowatości oraz innych defektów. Twardość warstw Ni+Al wynosiła około 240 HV, podczas gdy twardość warstw galwanicznych z czystego niklu wynosiła 220 HV. Zbadano wpływ obróbki cieplnej na formowanie się faz. Warstwy Ni+Al/Ni były przekształcane w warstwy kompozytowe γ -Ni+ γ' /Ni podczas wygrzewania w próżni w temperaturze 600°C przez 2 godziny oraz następnie w temperaturze 900°C przez 3 godziny pod naciskiem (ciśnienie prasowania około 1 MPa). Po obróbce cieplnej uzyskano nieporowate kompozytowe powłoki zawierające roztwór stały γ -Ni oraz fazę międzymetaliczną γ' (Ni₃Al). Zastosowana warstwa niklu skutecznie zablokowała dyfuzję pomiędzy podłożem z żelaza ARMCO oraz cząstkami aluminium i dlatego w badanych próbkach nie stwierdzono występowania kruchych faz z układu Fe-Al. Twardość warstwy γ -Ni+ γ' uzyskanej w wyniku syntezy faz wynosiła około 280 HV. Po teście wyżarzania w atmosferze utleniającej zauważono spadek twardości w wierzchnim obszarze warstwy do około 250 HV, co wynikało ze zmniejszenia się ilości fazy γ' . Na głębokości około 15 μ m zaobserwowano skokowy wzrost twardości do około 320 HV i stwierdzono w tym obszarze występowanie warstwy składającej się z tlenku aluminium.

Słowa kluczowe: warstwa kompozytowa γ -Ni/ γ' , współosadzanie sedymentacyjne, wyżarzanie, utlenianie

INTRODUCTION

Electrodeposition is a very simple and cost-efficient technique which is widely used to produce composite coatings for applications requiring wear and abrasion resistance. There are two types of electrodeposition techniques: conventional electrodeposition (CED), in which the anode and cathode are vertically inserted in

the bath and sediment co-deposition (SCD) developed by Viswanathan and Ghose [1], in which the anode and cathode are set horizontally. It has been recently demonstrated that composite coatings can contain hard ceramic particles (Al₂O₃, SiC, ZrO₂) and/or polymers (PTFE) in a metal matrix [2-4]. Another type of compo-

site coating can be produced by co-deposition of metallic particles into an electrodeposited matrix. So far, several coatings such as Ni-Cr developed by Bazzard and Boden [5], Ni-CrAlY developed by Honey et al. [6] and Ni-Al have been produced. Among these coatings, Ni-Al-based alloys have attracted considerable attention because of their great potential for high-temperature structural applications due to the low density, high strength at an elevated temperature and excellent resistance to high-temperature oxidation. Many investigators [7-10] developed γ -Ni+ β (NiAl)+ γ' (Ni₃Al) or γ -Ni+ γ' composites by annealing electrodeposited Ni-Al coatings, during which the co-deposited Al particles were converted into β or γ' phases by reaction with Ni. It is very profitable that the γ' phase (ordered fcc L1₂ structure) precipitates coherently in a γ -Ni (fcc structure) matrix [11]. Nickel and γ' have not only a similar structure, but also a modest lattice mismatch (with a lattice constant of 0.3524 and 0.3570 nm for Ni and γ' phase, respectively). The γ' precipitates exhibit a cube-on-cube orientation relationship with the Ni matrix, so that $(001)_{\gamma'}/(001)_{\gamma}$ and $[100]_{\gamma'}/[100]_{\gamma}$. There is a low strain energy associated with γ' /Ni interfaces lying on $\{100\}$ planes. During plastic deformation, dislocations in the Ni matrix prefer to cut through the γ' precipitates, rather than bypassing them. Therefore, according to Wang et al. [12] a γ -Ni+ γ' composite can behave as a ductile alloy with a high ultimate tensile strength and large elongation. Varma and Lebrat [13] found out that the morphological development of electro-co-deposited Ni-Al coatings during heat treatment was similar to that determined in the synthesis of bulk nickel aluminides by powder metallurgy. However, in electrodeposited coatings, the Al particles are effectively isolated from each other by the Ni matrix. At elevated temperatures, phase formation takes place locally around the individual particles. Many investigators [7, 9, 14] reported the presence of pores throughout the microstructure in γ -Ni/ γ' coatings, which were formed due to local density changes as the Al particles and Ni matrix transform to intermetallic phases.

The mechanical properties of the transition joints between the iron and electrodeposited Ni+Al films subsequently converted into γ -Ni+ γ' coatings, could be impaired by Fe-Al-based intermetallic compounds. The use of appropriate intermediate materials can minimise the formation of brittle intermetallics. In this context, nickel having a substantial solid solubility in iron seems to be a useful material.

The main purpose of this work was to produce fully dense γ -Ni+ γ' composite coatings on an iron substrate using nickel as an interlayer. The influence of the employed manufacturing method on the coating oxidation behaviour was also investigated.

EXPERIMENTAL PROCEDURE

Armco iron specimens of the following composition: C 0.034%, Mn 0.038%, S 0.021%, P 0.01% and Fe

balance, with the sizes of 20 x 20 x 2 mm were cut from a plate and then abraded with 1200-grit SiC waterproof paper. After being ultrasonically cleaned in acetone, the specimens were electrodeposited using the CED technique with a 15 μ m thick film of pure nickel from a Watt's type nickel bath containing 300 g/l NiSO₄·7H₂O, 50 g/l NiCl₂·6H₂O and 35g/l H₃BO₃. The used operating conditions were: current density 3 A/dm², temperature 35 °C and pH ~4.0. The anode was a pure electrolytic Ni (>99.9%) plate grounded with SiC paper to a 400-grit finish. After that, the specimens with as-plated Ni coatings were polished with a 1 μ m diamond suspension, cleaned in acetone and again electrodeposited using the SCD technique once, whose schematic diagram is shown in Figure 1.

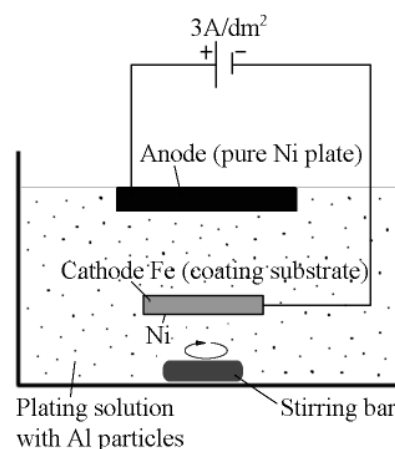


Fig. 1. Schematic diagram of used sediment co-deposition (SCD) technique

Rys. 1. Schemat zastosowanej metody współosadzania sedymentacyjnego

The composition of the bath and operating conditions were the same as previous. The bath additionally contained 40g/l of pure Al powder with an average particle size of 3 μ m. During SCD, the plating solution was magnetically stirred (250 rpm) in order to keep the particles dispersed and suspended in the electrolyte. The SCD plating time was 3 hours. After the deposition, some as-deposited samples were examined to determine the volume fraction of Al particles in the composite coatings. The remaining as-deposited specimens were heated in a vacuum furnace (at a vacuum level of 0.01 Pa) under uniaxial pressure of 1 MPa that was applied during diffusion treatments to reduce porosity. Firstly, the specimens were heated at a rate of 20°C/min to 600°C and soaked for 2 hours for the reaction synthesis. Subsequently, the temperature was increased to 900°C for rapid development of the structural processes. The samples were held at 900°C for 3 hours and then furnace-cooled naturally to room temperature. After that, the oxidation resistance of as-received γ -Ni+ γ' composite coatings was investigated. Oxidation tests were performed in static air at 1000°C. The samples were removed from the furnace after 20 hours and cooled to room temperature. For

characterisation, the specimens with as-plated Ni+Al/Ni coatings, specimens after diffusion treatment and specimens after oxidation tests were sectioned and mounted in a cold setting resin. Grinding was conducted with successively finer silicon carbide papers from 180 to 1200 grit. The polishing steps, including 6 and 1 μm diamond suspensions were performed using a Struers polishing machine. The microstructural observations were conducted using a JEOL JMS-5400 scanning electron microscope (SEM) and a Carl Zeiss NEOPHOT 2 optical microscope. The chemical composition of the phases was determined by comparing the results of the electron-probe microanalysis (EDS) obtained by means of an Oxford Instruments ISIS-300 system with the data in the binary Ni-Al phase diagram made by Baker [15] and with the data in the ternary Fe-Ni-Al system elucidated by Eleno et al. [16]. Vickers measurements were performed by a Hanemann microhardness tester mounted on a NEOPHOT 2 microscope under a load of 0.637 N for 15 s.

RESULTS AND DISCUSSION

A typical unetched Ni+Al/Ni composite coating is shown in Figure 2. The composite coating is uniform in its thickness, which was controlled to be about 15 μm for the Ni layer and about 100 μm for the SCD Ni+Al layer.

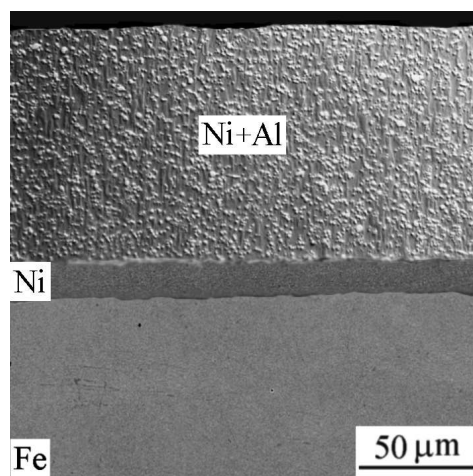


Fig. 2. Optical micrograph of as-plated Ni+Al/Ni coating
Rys. 2. Mikrostruktura osadzonej galwanicznie powłoki Ni+Al/Ni

Al particles are homogeneously distributed throughout the Ni+Al coating that contains about 25 vol.% Al and columnar nickel grains. No defects such as pores or cracks were observed in the as-plated Ni+Al/Ni coatings.

Details of the reaction synthesis of Ni+Al composite coatings have been provided by Izaki et al. [17]. The intermetallic phases formed concentrically around the original Al particles or at the Al/Ni interfaces. During heating at about 520°C, a β phase is formed by a rapid, exothermal reaction. Immediately after the reaction, the

coating microstructure consists of β particles in a Ni matrix with some Al in the solution. At higher temperatures, the γ' phase is formed between β and γ -Ni. The final coating morphology consists of blocks of γ' in a saturated γ -Ni solid solution matrix. Unfortunately, in bulk reaction synthesis, porosity is always found in the resultant microstructure. A significant amount of small pores within γ -Ni+ γ' composite coatings have been reported by Susan and Marder [7] and Liu and Chen [14]. The pores throughout the microstructure in the γ -Ni+ γ' coatings might be formed due to local densification as the Al particles and Ni matrix transform to intermetallics. The calculations show that a composite of 75 at.% Ni and 25 at.% Al that fully transforms to γ' should have about a 9% resultant porosity due to density changes. In addition, some pore formation may be accounted for the Kirkendall effect that occurs in the Ni-Al system, producing voids near the reaction interface during diffusion. A potential solution to the pore formation problem is applying pressure during the propagation stage of the reaction. Therefore in this investigation, as-plated samples were treated in a vacuum furnace under uniaxial pressure of 1 MPa (Fig. 3).

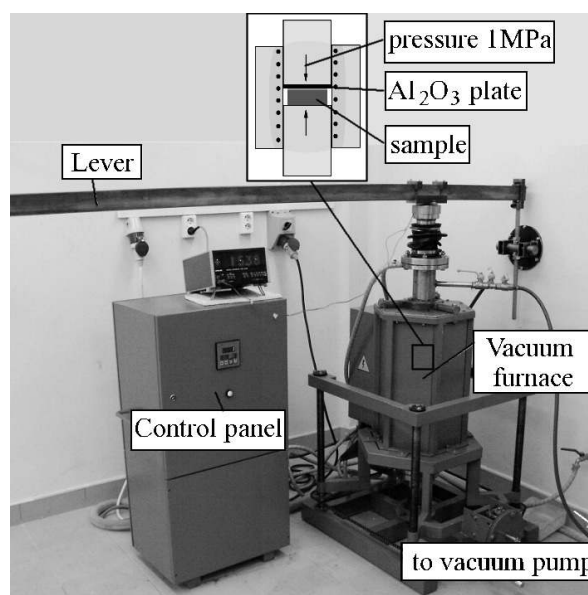


Fig. 3. Equipment used in the present study to form fully-dense composite coatings

Rys. 3. Urządzenia zastosowane do wytwarzania nieporowatych warstw kompozytowych

After electrodeposition and heat treatment under pressure, the fully dense composite coatings consist of a two-phase mixture with blocky morphology and a sublayer neighbouring to the iron substrate (Fig. 4).

Using X-ray microanalysis, it was found that the dark-grey single phase containing Ni (75.44 at.%) and Al (24.56 at.%) is the γ' intermetallic compound. The lightly shaded region that surrounds the γ' cuboidal particles consisting of Ni (92.47 at.%) and Al (7.53 at.%) is the γ -Ni solid solution. The EDS spectra for the

homogeneous regions of the reaction zone are presented in Figure 5.

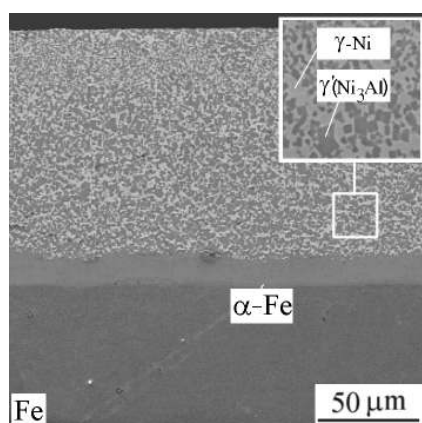


Fig. 4. SEM micrograph of annealed γ -Ni+ γ' /Ni coating after 2 h at 600°C and subsequently 3 h at 900°C

Rys. 4. Mikrofotografia warstwy γ -Ni+ γ' /Ni uzyskanej po wyżarzaniu przez 2 h w temp. 600°C oraz następnie przez 3 h w temp. 900°C uzyskana z zastosowaniem mikroskopu skaningowego

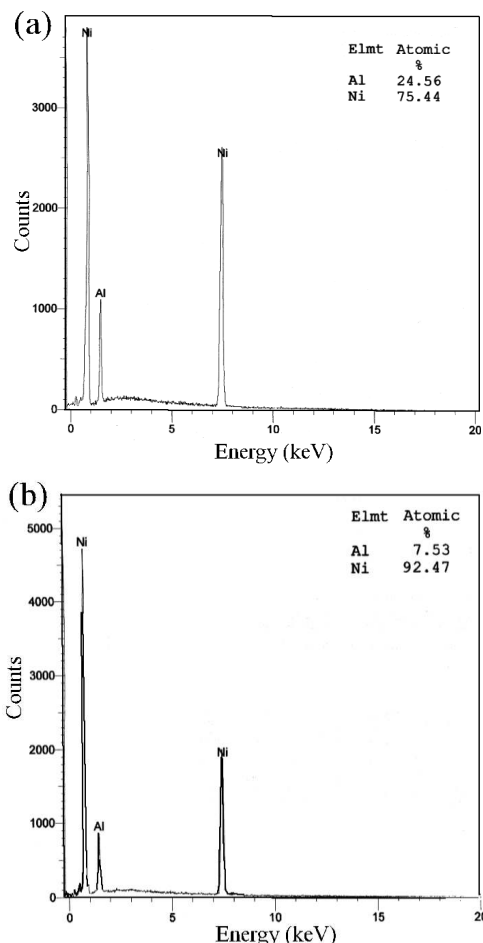


Fig. 5. Energy spectrum for emitted X rays for: (a) γ' and (b) γ -Ni regions

Rys. 5. Wyniki mikroanalizy rentgenowskiej dla: (a) fazy γ' oraz (b) obszaru zawierającego roztwór γ -Ni

As Qiu demonstrated [18], in coherent solids, the elastic strain energy associated with the misfit between the particle and the matrix structures has a strong influ-

ence on the development of both the particle morphology and the interparticle spatial correlation during coarsening. When the γ' particles are small and the misfit is negligible, the interfacial energy dominates the coarsening process. As a result, the particles take a spherical shape and are distributed randomly. When the γ' particles coarsen, the misfit becomes significant and the elastic strain energy dominates the coarsening process over the interfacial energy. As a result, the particles change from a spherical to cuboidal shape.

It is very important for composite coatings on an iron substrate to maintain a low concentration of Al, since Fe-Al-based brittle intermetallics could impair the mechanical properties of the Fe/coating boundary. X-ray microanalysis of the sublayer neighbouring to the Fe substrate (Fig. 6) shows that only solid solutions: α -Fe (showed in Fig. 4) and γ -Ni were formed.

It is evident from the study that a 15 μ m thick nickel interlayer can sufficiently block the diffusion of Al to the Fe side. The penetration of the Al atoms across nickel interlayer is very limited and the possibility of the formation of the brittle Fe-Al-based intermetallics is minuscule.

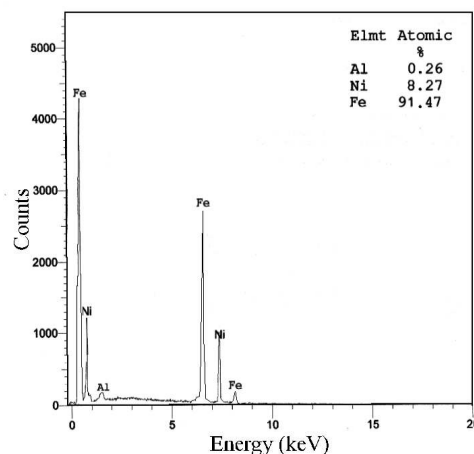


Fig. 6. Energy spectrum for emitted X rays for α -Fe solid solution

Rys. 6. Wynik mikroanalizy rentgenowskiej dla roztworu stałego α -Fe

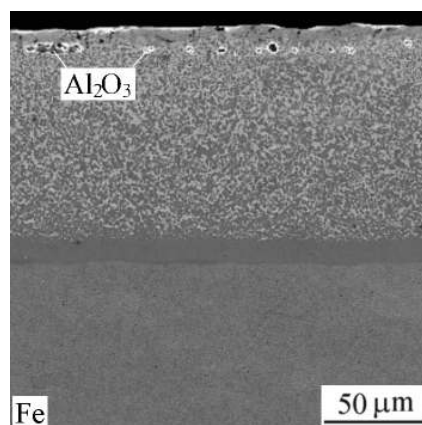


Fig. 7. Cross-sectional morphology of γ -Ni+ γ' /Ni coating after 20 h oxidation at 1000°C

Rys. 7. Struktura kompozytowej warstwy γ -Ni+ γ' /Ni po 20 h utleniania w temp. 1000°C

Figure 7 shows the microstructure formed after 20 hours oxidation at 1000°C. The outer layer (approx. 20 µm in thickness) exhibited a structure with a continuous layer of oxides in different sizes. EDS analysis of the oxides produced only Al and O peaks so they were qualitatively identified as an Al₂O₃ phase.

Microhardness measurements were conducted for the specimens with as-plated Ni+Al/Ni coatings, specimens after diffusion treatment and specimens after oxidation tests (Fig. 8).

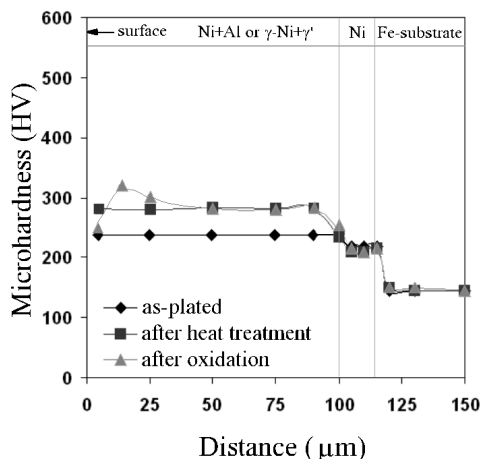


Fig. 8. Microhardness profiles across investigated specimens

Rys. 8. Zmiana mikrotwardości na przekrojach badanych próbek

The results of the microindentation hardness measurements showed that the as-plated Ni+Al coating (240 HV) was harder than the pure Ni interlayer (220 HV). The increase in hardness with the addition of soft Al particles could surprise, but similar results were obtained before also by Susan et al. [19]. It can be explained by the structural refinement of the Ni matrix when Al particles are added. When the Al particles are incorporated into a growing matrix, small Ni grains nucleate on the surface of the Al particles. Therefore, the hardening effect may be similar to the Hall-Petch type strengthening for a reduction in grain size. The results of hardness measurements after heat treatment showed that the hardness continuously decreased from the reaction-formed fully-dense γ -Ni+ γ' layer (280 HV) across the nickel sublayer (210 HV) to the iron substrate (145 HV). It confirmed the results of SEM investigations and EDS analysis showing that no hard nor brittle intermetallics were formed across the interface of γ -Ni+ γ' /Ni and Ni/Fe. The results for the specimens after oxidation tests showed that the microhardness near the surface decreased from 280 HV to about 250 HV, which might be attributed to the depletion of the γ' phase. A hardness peak of about 320 HV appeared at about 15 µm within the outer layer. In accordance with this result, SEM and EDS analysis revealed alumina particles there, as shown in Figure 7. After the peak, the hardness dropped to a stable level corresponding to the hardness of the γ -Ni+ γ' layer.

CONCLUSIONS

1. Ni+Al/Ni composite coatings on an iron substrate without cracking, porosity or other defects can be easily developed via two-step technology: conventional electrodeposition (CED) and sediment co-deposition (SCD).
2. The hardness of the Ni+Al composite coatings containing about 25 vol.% of Al is about 240 HV, whereas the hardness of the pure Ni coating is 220 HV.
3. The Ni+Al/Ni coatings can be converted into full-density γ -Ni+ γ' /Ni coatings by vacuum annealing at 600°C for 2 h and subsequently at 900°C for 3 h under uniaxial pressure of 1 MPa.
4. The hardness of the reaction-formed γ -Ni+ γ' layer is about 280 HV. The hardness near the surface after the oxidation tests decreases to about 250 HV, which is attributed to the depletion of the γ' phase. A hardness peak of about 320 HV appears at about 15 µm within the outer layer, where alumina particles were revealed.
5. The 15 µm thick nickel interlayer can sufficiently block the mutual diffusion between the iron substrate and aluminium particles, so hard and brittle Fe-Al-based intermetallics are not formed.

REFERENCES

- [1] Viswanathan M., Ghose M., Occlusion plating of nickel-graphite composite, *Metal Finishing* 1979, 77, 67-69.
- [2] Wang S.C., Wei W.C.J., Kinetics of electroplating process of nano-sized ceramic particle/Ni composite, *Materials Chemistry and Physics* 2003, 78, 574-580.
- [3] Szeptycka B., Hybrydowe niklowe powłoki elektrochemiczne Ni-SiC-PTFE, *Kompozyty (Composites)* 2001, 2, 137-140.
- [4] Trzaska M., Kucharska B., Wpływ gęstości prądu i składu kąpiel na właściwości warstw kompozytowych Ni/PTFE, *Kompozyty (Composites)* 2008, 8, 77-81.
- [5] Bazzard R., Boden P.J., Nickel-chromium alloys by co-deposition: Part I. Co-deposition of chromium particles in a nickel matrix, *Transactions of the Institute of Metal Finishing* 1972, 50, 63-69.
- [6] Honey F.J., Kedward E.C., Wride V., The development of electrodeposits for high-temperature oxidation/corrosion resistance, *Journal of Vacuum Science and Technology* 1986, 4, 2593-2597.
- [7] Susan D.F., Marder A.R., Ni-Al composite coatings: diffusion analysis and coating lifetime estimation, *Acta Materialia* 2001, 49, 1153-1163.
- [8] Konieczny M., Mola R., Properties of Ni-intermetallic phases coating deposited on C45 steel, *Hutnik - Wiadomości Hutnicze* 2004, 7-8, 362-363.
- [9] Yang X., Peng X., Wang F., Size effect of Al particles on structure and oxidation of Ni/Ni₃Al composites transformed from electrodeposited Ni-Al films, *Scripta Materialia* 2007, 56, 509-512.
- [10] Zhou Y.B., Zhao G.G., Zhang H.J., Zhang Y.C., Qian B.Y., Effect of CeO₂ on the microstructure and isothermal oxidation of Ni-Al alloy coatings transformed from electrodeposited Ni-Al films at 800°C, *Vacuum* 2009, 83, 1333-1339.
- [11] Alman D.E., Dogan C.P., Hawk J., Rawers J.C., Processing, structure and properties of metal-intermetallic layered com-

- posites, *Materials Science and Engineering A* 1995, 192-193, 624-632.
- [12] Wang H., Han J., Du S., Northwood D.O., Reaction synthesis of nickel/aluminide multilayer composites using Ni and Al foils: microstructures, tensile properties and deformation behaviour, *Metallurgical and Materials Transactions* 2007, A38, 409-419.
- [13] Varma A., Lebrat J.P., Combustion synthesis of advanced materials, *Chemical Engineering Science* 1992, 47, 2179-2194.
- [14] Liu H., Chen W., Electrodeposited Ni-Al composite coatings with high Al content by sediment co-deposition, *Surface and Coating Technology* 2005, 191, 341-350.
- [15] Baker H., *ASM Handbook*, Materials Park, OH, 3, 249.
- [16] Eleno L., Frisk K., Schneider A., Assessment of the Fe-Ni-Al system, *Intermetallics* 2006, 14, 1276-1290.
- [17] Izaki M., Fukusumi M., Enomoto H., Omi T., Nakayama Y., High-temperature oxidation resistance of Ni-Al films prepared by heating electrodeposited composite, *Journal of Japan Institute of Metals* 1993, 57, 182-189.
- [18] Qiu, Y.Y., Retarded coarsening phenomenon of γ' particles in Ni-based alloy, *Acta Materialia* 1996, 44, 4969-4980.
- [19] Susan D.F., Barmak K., Marder A.R., Electrodeposited Ni-Al particle composite coatings, *Thin Solid Films* 1997, 307, 133-140.